

Liquid Structure of *N,N*-Dimethylformamide, Acetonitrile, and Their 1:1 Molar Mixture

Tamas RADNAI,^{††} Sumiko ITOH, and Hitoshi OHTAKI^{*,†}

Department of Electronic Chemistry, Tokyo Institute of Technology at Nagatsuta,
4259 Nagatsuta, Midori-ku, Yokohama 227

(Received May 12, 1988)

Liquid structures of pure *N,N*-dimethylformamide (DMF) and acetonitrile (AN) as well as of their 1:1 molar mixture were investigated by X-ray diffraction at 25 °C. The careful reinvestigation of pure DMF led to a good reproducibility of the previous result. Slight deviations in the structural parameters are discussed and a detailed parameter table is reported. A simple model in which each AN molecule has 2 neighbors at an average distance of 330 pm describes the more ordered first neighbor structure of pure AN. The main interaction forming the structure is of dipole–dipole type, in agreement with previous findings. In the 1:1 molar mixture a dipole–dipole model also leads to a satisfactory description of the first neighbor structure. The preferred orientation is that with dipoles in the antiparallel position. A central DMF molecule has 1.75 neighboring AN molecules in average at a distance of 316 pm. The same stands for DMF around AN. No evidence for other kinds of interaction, e.g., weak H-bond type intermolecular interactions could be found in the mixture.

Both *N,N*-dimethylformamide (DMF) and acetonitrile (AN) are typical aprotic, dipolar, simple organic solvents. They are widely used in the chemical practice due to their advantageous physicochemical properties like the broad temperature range in which they are liquid; relatively high dielectric constants as well as good donor and acceptor properties which enable them to be excellent solvents for a great number of compounds. Their basic physical and chemical properties are often subjects of studies.

Recently, their liquid structure was also a matter of investigations.^{1–4} An X-ray diffraction study of liquid DMF revealed the intramolecular structure,¹⁾ while no direct evidence could be found for ordering effects between the molecules. The joined MO calculations suggested a slight tendency for dimer formation, but the interactions between the molecules were found to be weak. Generally acetonitrile is also considered as a structureless liquid, because of the lack of H-bonds, in spite of the appearance of the definite short range ordering between the molecules. The ordering is mainly due to the dipole–dipole interactions, as derived from diffraction and theoretical studies.^{2–4}

Surprisingly enough, the properties of the binary mixtures of DMF and AN have not been studied extensively. They are miscible at any concentration, forming non-azeotropic mixtures, but no detailed data of the physicochemical properties as well as their structures are available up to now. It is generally assumed that the solvent structural effects are very weak and can be neglected when compared with solute–solvent interactions in their binary solutions.

Some indications, however, point to the existence of molecular associations between DMF and AN in mix-

tures. Comparing Gutmann's donor and acceptor numbers of the two solvents, one can conclude that a remarkable difference is in the donicity ($D_N(\text{AN})=14.1$, $D_N(\text{DMF})=26.6$), while the acceptor numbers are similar ($A_N(\text{AN})=19.3$, $A_N(\text{DMF})=16.0$). These differences lead to variations in the metal–ligand complex formation as well as to differences in the solvation of the metal ions in the pure solvents. Moreover, the solvation and complex formation phenomena can also be affected in the mixtures. Indeed, it was proved that a preferential solvation of copper(II) ions by DMF occurs in the mixtures of DMF and AN when studying the $[\text{CuCl}_n]^{(2-n)+}$ complex formation.⁵ It is obvious to think that the differences in their donor and acceptor properties can also lead to a measurable degree of DMF–AN complex formation, even if the governing interaction is weak.

Literature data also support the hypothesis. Evidence of attractive interactions between DMF and AN is reported on the basis of light scattering studies.⁶ These interactions are in competition with the ones between the like molecules and a great number of single molecules have also to be present in the liquid, according to the measured excess free energy data. More direct evidence for solute–solute type interactions between DMF and AN as solutes even at low concentrations in benzene solutions was found by the dielectric relaxation method⁷⁾ practically at every stoichiometric ratio of the solutes. In a previous work, however, from electro-osmotic measurements the weakness of such interactions, if any, was emphasized.⁸⁾ Indeed, guesswork on possible type of interactions suggests weak H-bond-like interactions between CH group of DMF and N atom of AN, and electric multipole–multipole interactions between the two kinds of molecules.

In order to determine the structural consequences of such presumed interactions, an X-ray diffraction measurement was performed on the 1:1 molar mixture of DMF and AN. For the sake of comparison, X-ray

[†] Present address: Coordination Chemistry Laboratories, Institute for Molecular Science, Myodaiji-cho, Okazaki 444.

^{††} On leave from: Central Research Institute for Chemistry of the Hungarian Academy of Sciences, Budapest, P.O.B.17, H-1525, Hungary.

measurements on pure DMF and AN were also carried out, and their structural data were compared with those reported in the literature.

Experimental

Sample Solutions. Both DMF and AN of reagent grade were distilled twice before use. A mixture of 1:1 molar ratio, corresponding to 1:1.781 mass ratio, was prepared by measuring the weights of the components. Densities of the samples were checked pycnometrically.

X-Ray Scattering Measurements. The scattering experiments were carried out with a JEOL θ - θ diffractometer by using Mo $K\alpha$ radiation ($\lambda=71.07$ pm) and a bent LiF monochromator in a room thermostated at $(25 \pm 1)^\circ\text{C}$. The accessible range of scattering angle (2θ) was 2 – 140° , corresponding to the s -range from 0.006 pm $^{-1}$ to 0.168 pm $^{-1}$, s being the scattering variable ($s=4\pi\lambda^{-1}\sin\theta$). Times requiring to accumulate 80000 counts were recorded at each angle of the measurements. Special care was taken of the low X-ray absorption as well as the high evaporation rates of the samples. The levels of the horizontal surface of the liquids were checked every 2–3 hours. Additionally, the low-angle region for the mixture and the whole experiment for the AN were measured repeatedly in order to obtain better results for data reduction. A typical result for the agreement between the data from two consecutive experiments was within 2–3%, and the deviation never exceeded 5%.

Beyond the above specialities, the method of measurements and data treatments were the same as those described in previous papers.⁹⁾

Analysis of the Scattering Data. Experimental intensities were corrected for background, absorption, double scattering, polarization and incoherent scattering by the standard methods. The reduced intensities $i(s)$ were calculated as:

$$i(s) = KI(s) - \sum n_j \{ [f_j(s) + \Delta f_j']^2 + (\Delta f_j'')^2 \}, \quad (1)$$

where $I(s)$ is the experimental intensity and is normalized to the absolute scale with respect to a stoichiometric volume V containing one DMF and AN molecule in the pure liquids, and one molecule of both kinds in the mixture, K is the normalizing factor, n_j is the number of atom j in the stoichiometric volume, $f_j(s)$ is the scattering factor of atom j at s , $\Delta f_j'$, and $\Delta f_j''$ are the real and imaginary parts of anomalous dispersion of atom j . The experimental radial distribution functions $D(r)$ and pair-correlation functions $G(r)$ were calculated by the Fourier transform of the $i(s)$ functions according to

$$D(r) = 4\pi r^2 \rho_0 + (2r/\pi) \int_0^{s_{\max}} si(s)M(s)\sin(sr)ds, \quad (2)$$

and

$$G(r) = D(r) / (4\pi r^2 \rho_0), \quad (3)$$

where ρ_0 denotes the average electron density in the sample defined as

$$\rho_0 = \sum \sum n_j n_i f_i(0) f_j(0) / V. \quad (4)$$

$M(s)$ is the modification function of the form

$$M(s) = \frac{\sum \{ [f_i(0) + \Delta f_i']^2 + (\Delta f_i'')^2 \}}{\sum \{ [f_N(s) + \Delta f_N']^2 + (\Delta f_N'')^2 \} \exp(-ks^2)}. \quad (5)$$

All calculations were performed by using appropriate versions of programs KURVLR¹⁰⁾ and NLPLSQ.¹¹⁾

Results and Discussion

Method of Structural Analysis. At first, a semi-quantitative analysis was done for each sample at the radial distribution level. $D(r)$ and $G(r)$ functions for DMF and AN were compared with those available from the literature, and the differences in the $D(r)$ functions of the three samples were discussed. As a second step, the intramolecular structural parameters for both DMF and AN were calculated by the least squares method (LSQ) at the reduced intensity level. Then models for intermolecular interactions were tested, trying to find the average configuration of the nearest neighbors by LSQ. When building up the model for the mixture, the parameters fixed previously in the LSQ analysis for the pure liquids were used for describing the intramolecular structure without changing them. Finally, the structural parameters for the random distribution of the atoms around the central ones were determined.

For the LSQ, theoretical reduced intensities $i_{th}(s)$ were calculated as

$$i_{th}(s) = \sum \sum n_{pq} c_{pq} j_0(sr_{pq}) \exp(-b_{pq}s^2) - 4\pi\rho_0 / s \sum \sum n_p n_q c_{pq} R_{pq}^2 j_1(sR_{pq}) \exp(-B_{pq}s^2). \quad (6)$$

where

$$c_{pq}(s) = \{ [f_p(s) + \Delta f_p'] [f_q(s) + \Delta f_q'] + \Delta f_p'' \Delta f_q'' \} M(s), \quad (7)$$

and r_{pq} , b_{pq} , and n_{pq} denote the distance, temperature factor, and frequency factor (coordination number) of the p - q atom-pair, respectively. R_{pq} is the distance beyond which a continuous distribution of atoms of type q around the p type atom in the center is assumed, while B_{pq} is the parameter describing the sharpness of the boundary at R_{pq} . For brevity, $j_m(x)$ stands for the spherical Bessel function of the m th order.

$$U = \sum_{s_{\min}}^{s_{\max}} \omega(s) [i(s) - i_{th}(s)]^2, \quad (8)$$

The LSQ procedure was applied in order to find the minimum of the error-square sum using the weighting functions $\omega(s)=s^2$. During the fitting procedure several s ranges were tried. Finally an extended range from $s_{\min}=0.005$ pm $^{-1}$ to $s_{\max}=0.16$ pm $^{-1}$ could be applied. The quality of the fit was checked through the value of U and the usually defined Hamilton R -factor.

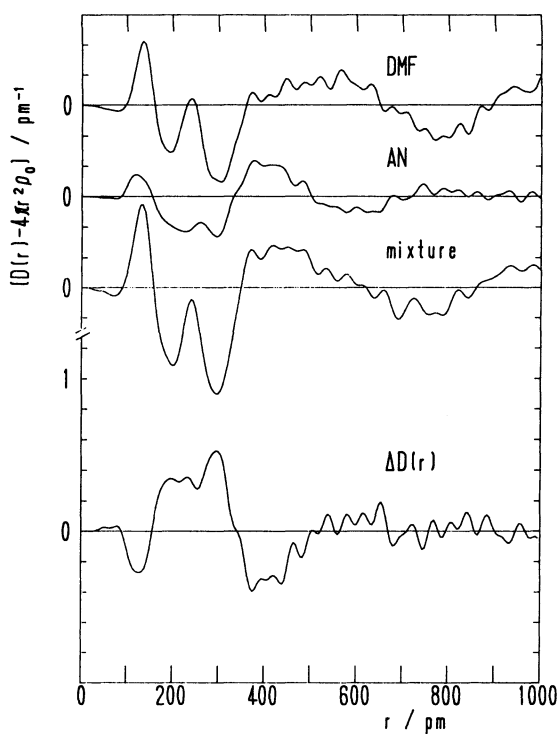


Fig. 1. Experimental RDF's for pure DMF, AN, their 1:1 molar mixture, and the weighted difference of the three curves. The RDF's are given in form of $D(r) - 4\pi r^2 \rho_0$, the difference curve as defined in Eq. 9.

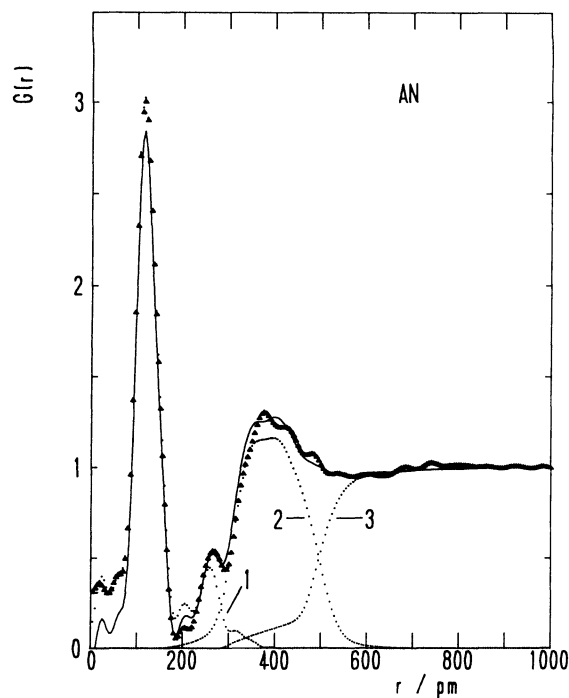


Fig. 3. Experimental $G(r)$ (triangles) is compared with the theoretical one from the best fit of the models (solid line) for pure AN. The dotted curves are: intramolecular contribution (1), intermolecular part from dipole-dipole model (2), and the continuum (3).

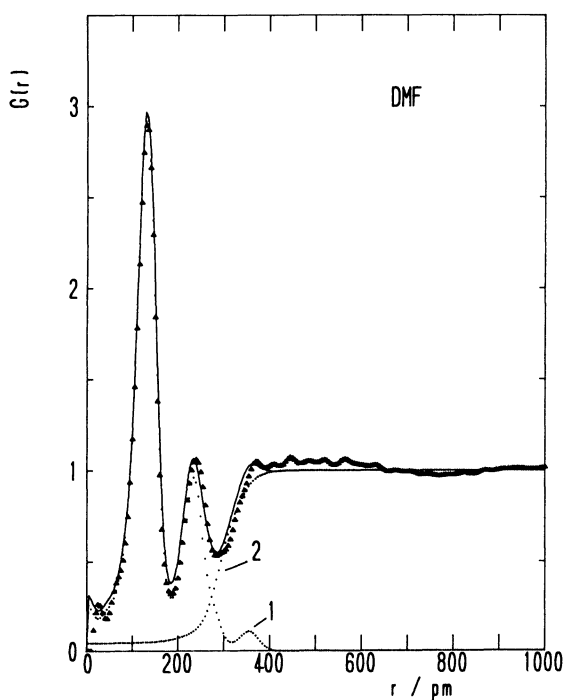


Fig. 2. Experimental $G(r)$ (triangles) is compared with the theoretical one from the best fit of the models (solid line) for pure DMF. The dots represent the intramolecular (1) and the continuum (2) contributions.

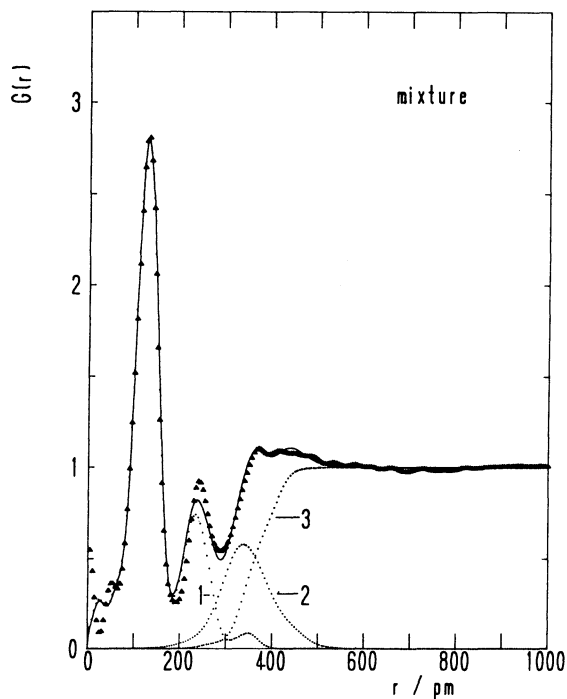


Fig. 4. Experimental $G(r)$ (triangles) is compared with the theoretical one from the best fit of the models (solid line) for 1:1 molar mixture of DMF and AN. The dotted curves are: intramolecular contribution (1), intermolecular part from the complete dipole-dipole model (2), and the continuum (3).

X-Ray Radial Distribution Functions (RDF's). The total experimental X-ray radial distribution curves of the three samples are shown in Fig. 1 in the form of $D(r)-4\pi r^2\rho_0$. The corresponding $G(r)$ functions are also shown in Figs. 2–4.

The two distinct peaks at about 130 and 230 pm for pure DMF were ascribed to the intramolecular interactions in a previous paper.¹⁾ The peak positions are very well reproduced in the present work (the resolution of the RDF was 5 pm, the agreement is within this limit). The peak shapes also agree well, except the small ripples which still remained after that a correction had been applied to remove them as far as possible. Since only a small modulation appears from 350 to 650 pm, it witnesses about the absence of any significant interaction between the molecules.

There are also two distinct peaks at about 120 and 270 pm on the RDF of pure AN, with a small peak at about 200 pm (see Fig. 1). The last one emerges as a hump at the corresponding $G(r)$ in Fig. 3. The peak positions and their relative heights are in good agreement with those reported earlier.²⁾ It is obvious to ascribe these three peaks to the intramolecular distances, similar to the DMF case. The peak appearing between 300 and 500 pm is less broad and significantly higher than that of DMF. It also has a shoulder at about 320 pm, and its shape is rather complex, reflecting stronger intermolecular interactions and as a consequence, more definite short-range ordering in the liquid.

The two main peaks in the RDF of the 1:1 molar mixture obviously include the intramolecular distances both from DMF and AN. Consequently, they become broader and the peak positions are shifted from those of pure liquids. As for the peak beyond to 300 pm, it is more definite than that for pure DMF, but less pronounced than for pure AN. It seems to be rather complex, and a more quantitative analysis is needed in order to decide if it reflects only the concentration effect, i.e., the simple mixing of the AN-like and DMF-like structures (which is physically not relevant) or is a sign of a specific interaction between the two kinds of molecules.

The first step towards the solution of this problem was the construction of the weighted difference of the experimental RDF's according to

$$\Delta D(r) = [D_M(r) - 4\pi r^2 \rho_{0,M}] - K_1[D_{DMF}(r) - 4\pi r^2 \rho_{0,DMF}] - K_2[D_{AN}(r) - 4\pi r^2 \rho_{0,AN}], \quad (9)$$

where $K_1 = \rho_{0,M}/\rho_{0,DMF}$, $K_2 = \rho_{0,M}/\rho_{0,AN}$ are two weights which account for the differences in the average atom densities between the samples (M stands for the mixture). The $\Delta D(r)$ curve is shown in Fig. 1. It is easy to prove that the function defined by Eq. 9 tends to zero when r is beyond the boundaries of the

continuum. Accordingly, the ripples beyond 600 pm are clearly spurious, summing up the experimental errors after the double subtractions and determine the accuracy of the peak resolution. On the other hand, the minimum and the maximum found in the intramolecular range up to 250 pm are also physically irrelevant, and are due to the enlarged errors from the inaccuracy of the ripple correction in the low- r range. The interesting feature of this difference curve is the sharp peak near 300 pm followed by a deep minimum around 380 pm. Both are larger than those found to be irrelevant, and give a clear indication not only for the presence of the intermolecular interaction between the molecules but also a detectable shift in the average interatomic distances between adjacent molecules towards the lower- r region.

Structure of Pure DMF. In spite of the visibly good agreement between the new and the previously reported experimental results, a detailed LSQ analysis of the $i(s)$ curve was carried out in order to see the influence of minor experimental deviations on the structural parameters. The planar structure for the DMF molecule was retained. In the structural model examined in the present study only two slight modifications were applied. The non-bonding C...H distances were not neglected in the fitting procedure although they give only small contributions to the X-ray scattering, and the treatment of the continuum (the second term in Eq. 6) was employed by separated atom-atom contributions of each kind of atoms (this latter change does not influence the intramolecular parameters).

The experimental and theoretical $si(s)$ functions of

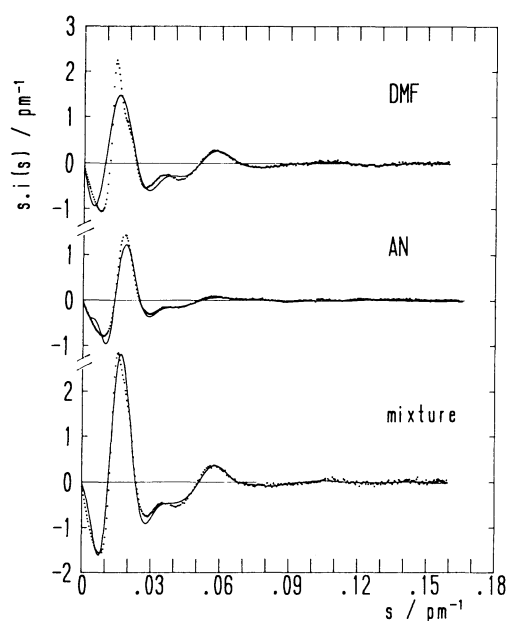


Fig. 5. Experimental structure functions $si(s)$ (dots) are compared with the theoretical ones from the best fit of the models (solid lines) for pure DMF, AN, and their 1:1 molar mixture.

Table 1. Intramolecular Parameters for Liquid DMF

Interaction	This work		Ref. 1		Ref. 12	
	<i>r</i>	<i>b</i> /10	<i>r</i>	<i>b</i> /10	<i>r</i>	<i>b</i> /10
C-H	109(1)	1(1)	109(1)	1(1)	—	—
C ₁ =O	124(2)	3(1)	124(2)	3(1)	120(1)	3(1)
C ₁ -N	135(2)	5(1)	135(2)	5(1)	140(1)	4(1)
C ₂ -N	145(2)	5(1)	145(2)	5(1)	143(1)	4(1)
N...H	202(2)	5(1)	202(2)	5(1)	—	—
O...H	202(2)	5(1)	203(2)	5(1)	—	—
N...H	207(3)	5(1)	208(2)	5(1)	—	—
O...N	235(5)	2(1)	225(3)	2(1)	231(2)	3(2)
C ₁ ...C ₂	238(5)	2(1)	239(5)	2(1)	247(3)	1(1)
C ₂ ...C ₃	261(5)	2(1)	257(5)	2(1)	244(2)	1(1)
C ₂ ...O	281(5)	5(2)	270(5)	5(2)	285(2)	1(1)
C ₃ ...O	358(5)	10(3)	354(5)	10(3)	359(5)	7(2)
C ₃ ...H	238(5)	2(2)	—	—	—	—
C ₂ ...H	331(5)	6(5)	—	—	—	—
<NC ₁ O	130		121		127	
<C ₁ NC ₂	116		116		121	
<C ₂ NC ₃	129		128		121	

a) Distances (*r*) in pm, and temperature factor (*b*) in pm². The calculated bond angles are also given (in degrees). The numbering of the atoms is the same as in Ref. 1 and is shown in Fig. 6.

Table 2. Parameters Describing the Continuum Parts of the Structure in Liquid DMF, AN, and Their 1:1 Molar Mixture

Atom pair	DMF		AN		Mixture	
	<i>R_{pq}</i>	<i>B_{pq}</i> /10	<i>R_{pq}</i>	<i>B_{pq}</i> /10	<i>R_{pq}</i>	<i>B_{pq}</i> /10
C-C	290(9)	18(2)	285(4)	109(44)	337(2)	40(5)
C-N	269(9)	37(3)	505(15)	18(5)	378(3)	37(3)
C-O	311(9)	36(4)	—	—	395(36)	36(9)
N-N	—	—	479(29)	6(2)	396(75)	38(19)
N-O	—	—	—	—	419(100)	4(4)

a) The contributions were calculated in an atom-atom distribution form. The boundaries of the continuum parts (*R_{pq}*) are given in pm, the corresponding *B_{pq}* values in pm².

the best fit are shown in Fig. 5. The intramolecular structural parameters for DMF are given in Table 1. As it is seen from the comparison with those parameters reported earlier,¹¹ no change occurred in the bonding distances, and only minor changes resulted in the nonbonding distances, leading to slight variation in the bond angles. For a further comparison, structural parameters derived from an independent X-ray study on pure DMF,¹² applying transmission geometry, are also given in Table 1. Although these structural parameters are somewhat different, but not contradictory to the results reported here.

The intermolecular part of the liquid structure of DMF is completely described by assuming random distribution of atoms around the central ones beyond to the boundaries given by the set of *R_{pq}* and *B_{pq}* parameters listed in Table 2. Only the C-C, C-N, and C-O contributions were fitted because of their major weights. The parameters obtained support the internal consistency of the model.

Structure of Pure AN. Intramolecular structural

parameters for liquid AN were determined earlier from X-ray diffraction experiments.^{2,3} Since there are slight differences between them, these parameters were also recalculated during the structural analysis. The values finally accepted are compared with the literature data in Table 3. No significant change in the intramolecular parameters was observed.

As for the intermolecular structure, the previous works employed two completely different approaches. The first one² interpreted the liquid structure in crystallographic terms, computing all possible interactions between eight molecules within an orthorhombic unit cell, and determining a "correlation-cluster" size resulting in a diameter of about 1300 pm. The molecules are arranged in the clusters with the parallel or antiparallel position of their dipoles. Although a decrease in the positional and orientational correlations was considered in the model, the ordering seems still to be exaggerated.

The other approach^{3,4} had the aim at determining the molecular pair-correlation function of liquid AN from combined neutron and X-ray diffraction exper-

Table 3. Intramolecular Parameters for Liquid AN

Interaction	This work		Ref. 2		Ref. 3	
	<i>r</i>	<i>b</i> /10	<i>r</i>	<i>b</i> /10	<i>r</i>	<i>b</i> /10
C'-H'	109(1)	1(1)	109	—	—	—
C'-C''	147(2)	1.7(3)	146.5(1)	2.7(3)	148(3)	3(1)
C'-N'	115(1)	1.6(3)	115.3(1)	1.4(1)	114(3)	4(1)
C''...N'	262(2)	5(1)	261.8(2)	4.1(2)	—	5(1)
C'...H'	208(3)	5(1)	—	—	212(3)	4(2)
N'...H'	314(3)	10(5)	—	—	—	8(1)

a) Distances (*r*) in pm, and temperature factor (*b*) in pm². The numbering of the atoms is given in Fig. 6.

iments. From the total experimental pair-correlation function and calculations by the perturbation theory combined with it, the leading terms of the invariant series expansion could be derived, characteristic to the positional and also the orientational correlations between the molecules. This information is much more beyond to that which is accessible only by one diffraction experiment. The results showed that the dipole-dipole and quadrupole-quadrupole interactions were essential at small intermolecular distances and that the antiparallel orientation of the dipoles was preferred. The average configuration of the first neighbors, however, was not given in terms of structural parameters.

In order to derive the simplest possible model for the first-neighbor structure of AN, an LSQ analysis was carried out. In the applied model two neighbors were assumed around a central molecule, with their dipoles in the antiparallel position. The separation distance *l* between the centers of the molecules was a fitted parameter, together with the *b* values rendered to the interatomic distances. Beyond the first neighbors, a random distribution of atoms was assumed. The agreement between the experimental and theoretical *si(s)* functions is shown in Fig. 5, and the corresponding *G(r)* curves in Fig. 3.

As a result of the fit, a separation distance between the neighboring molecules *l*=330 pm was obtained. This value agreed well with that of 335 pm which can be calculated from the coordinates of atoms in the unit cell given in Ref. 2. Beyond the two nearest neighbors no more molecules were needed to obtain a good fit, and random distribution of atoms was enough to describe the remaining structure.

Intermolecular Structure of the Mixture. Since the analysis of the RDF's suggested that structural effect may occur when mixing the two pure solvents, a detailed LSQ analysis of the *i(s)* for 1:1 molar mixture was also carried out. Various model combinations were tested. At first, a rough estimate gave the average number of 5.5 for N or C atoms at about 330 pm distant from a central one. Similarly, 8.7 N or C atoms were found around a central O atom at a distance of about 380 pm. This result would correspond to 2.7—2.9 AN molecules around a central DMF molecule. Of course, this picture is very rough, since it does not

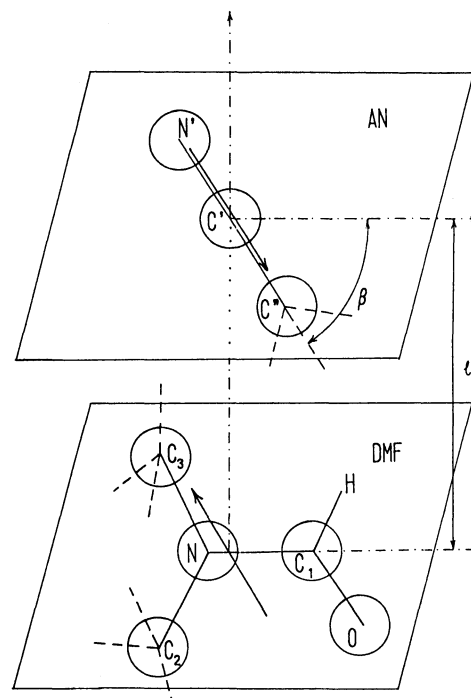


Fig. 6. Schematic drawing of the structural model for DMF-AN complexes. For the sake of simplicity, only one DMF and one AN molecules are shown, the unlike molecules above and below should be arranged accordingly. The direction of the dipoles of the molecules are indicated by arrows. The numbering of the atoms is also shown (primes always refer to atoms belonging to AN). The H atoms of the methyl groups are indicated by dashed lines.

distinguish between the types of atoms and does not specify any geometry for the structure. Correspondingly, the fit was not satisfactory enough.

As a second step, a complete model was constructed. From the results of pure AN it was supposed that the dominant interaction between DMF and AN molecule is via their dipoles. The idea for formulating the model was that while retaining the nearest neighbor model for pure AN, the central molecule should be changed to a DMF one in the mixture. The DMF molecule was allowed then to change its orientation to construct various types of the DMF-AN complex. Figure 6 shows the schematic drawing of the model and defines the structural parameters included. It was

Table 4. Calculated Intermolecular Distances (in pm) and b Values (in pm²) between the Neighboring DMF and AN Molecules from the Best Fit for the 1:1 Molar Mixture

Interaction	r	$b/10$
C'...N	317	51(7)
N'...C ₃	319	167(20)
C''...O	329	40(10)
N'...N	332	167(20)
C'...C ₁	332	51(7)
C''...C ₁	341	40(10)
C'...C ₂	355	51(7)
C'...C ₃	355	51(7)
C''...N	356	40(10)
C''...C ₂	361	40(10)
N'...C ₁	369	167(20)
C'...O	373	51(7)
N'...C ₂	391	167(20)
N'...O	439	167(20)
C''...C ₃	441	40(10)

supposed that the axis of the two molecules lay in parallel planes, and their centers lay on a line perpendicular to the planes. Independent parameters for the fit were: the number n of AN molecules around the central DMF, which corresponds to a set of equal atomic coordination numbers by definition, the separation distance l between the centers of the molecules, corresponding also to a set of atom-atom distances; the rotation angle β around the l -axis, and three b_{ij} values where i and j indicate different molecules. Continuum parameters for each kind of atom-pairs were also included in the fit, but later the terms of less importance (those containing H atoms) were excluded. The interactions of the central DMF molecules with those molecules which are at a distance larger than l , e.g., being within the same plane, were considered in the continuum part. This model obviously has some-rather arbitrary-restrictions, but the requirement of using the least number of structural parameters was always kept in mind during the calculations.

The corresponding pair-correlation functions $G(r)$ and the structure functions $si(s)$ after reaching the best fit are shown in Figs. 4 and 5, respectively. Table 4 shows the (dependent) interatomic distances between DMF and AN molecules calculated from the best fitted independent parameters. Parameters for describing the continuum are given in Table 2.

The final values of $n=1.75\pm0.08$, $l=316\pm20$ pm, and $\beta=59\pm10$ degree were obtained. The number of AN molecules around a central DMF molecule being somewhat less than 2 seems to be reasonable, because the structure of the DMF-AN mixture, in which a half of AN molecules in the pure state are replaced to DMF molecules, may have a similar, but slightly disordered molecular arrangement, to the pure liquid of AN. For a further consideration, the whole procedure was

repeated when an AN molecule was placed in the middle. Similarly, a number of $n=1.86\pm0.1$ DMF molecules were determined to be around the AN.

The obtained value for the rotation angle β corresponds to the antiparallel orientation of the dipoles. The least squares sum, in fact, was not very sensitive to the variation of β alone. The R -factor change only about 10% when β varied from 0 to 60 degrees. The only sharp increase in R -factor occurred, amounting up to 300% of the minimum value obtained when the unfavorable parallel orientation was tested.

It is very interesting to note that the separation distance l proved to be less than between two neighboring molecules in pure AN. Its shift from 330 pm to 316 pm going from the pure liquid to the mixture is meaningful, without doubt. It is also noteworthy that when letting to vary l and β together, the favorable antiparallel orientation occurred by accompanying a decrease in the separation distance. It can not be concluded from this fact directly, however, that the interaction between the DMF and AN is stronger than between two AN molecules, but only that the yielded configuration is sterically the most favorable. This may be due to the fortunate coincidence of a more bulky, basically planar DMF molecule with a smaller, and essentially linear AN molecule. For determining the strength of interactions more extended, energetic studies are needed with more appropriate methods.

Several additional tries for finding evidence for other kinds of possible first neighbor configurations were also carried out, but all they failed. Especially when searching for contributions due to weak H-bond type interactions between CH groups of DMF and N atoms of AN at about their characteristic distance of 290–310 pm, no noticeable finding was obtained. The LSQ fit could not be improved, and no remaining peak in the radial distribution function could be observed in the given range neither before constructing the H-bond type model, nor looking for some minor contribution still to be considered after the complete model had been applied.

The work has been supported, in part, by the Ministry of Education, Science and Culture (Grant-in-Aid for Scientific Research on Priority Area of Macromolecular Complexes, No. 62612005). One of us (T.R.) is greatly indebted to the Tokyo Institute of Technology and the Hungarian Academy of Sciences to allow for being engaged into the present study. Computers at the Tokyo Institute of Technology were used for the calculations.

References

- 1) H. Ohtaki, S. Itoh, T. Yamaguchi, S. Ishiguro, and B. M. Rode, *Bull. Chem. Soc. Jpn.*, **56**, 3406 (1983).

- 2) A. Kratochwill, J. U. Weidner, and H. Zimmermann, *Ber. Buns. Ges.*, **77**, 408 (1973).
 - 3) H. Bertagnolli and M. Zeidler, *Mol. Phys.*, **36**, 177 (1978).
 - 4) O. Steinhauser and H. Bertagnolli, *Chem. Phys. Lett.*, **78**, 555 (1981).
 - 5) S. Ishiguro and H. Ohtaki, *J. Coord. Chem.*, **15**, 237 (1987).
 - 6) I. Katime and L. C. Cesteros, *J. Chem. Soc., Faraday Trans. 2*, **80**, 1215 (1984).
 - 7) A. K. Sharma, D. R. Sharma, and D. S. Gill, *J. Phys., D*, **18**, 1199 (1985).
 - 8) R. L. Blokhra, M. L. Parmar, and S. K. Agarval, *J. Electroanal. Chem.*, **89**, 417 (1978).
 - 9) See e.g., H. Ohtaki, M. Maeda, and S. Ito, *Bull. Chem. Soc. Jpn.*, **47**, 2217 (1974) or H. Ohtaki, T. Yamaguchi, and M. Maeda, *Bull. Chem. Soc. Jpn.*, **49**, 701 (1976).
 - 10) G. Johansson and M. Sandström, *Chem. Scr.*, **4**, 195 (1973).
 - 11) T. Yamaguchi, Doctor Thesis, Tokyo Inst. of Technol., March (1983).
 - 12) I. Serke, Doctor Thesis, Central Res. Inst. of Hung. Acad. Sci., (1983).
-